Food Chemistry 111 (2008) 663–675

Contents lists available at ScienceDirect

Food Chemistry

journal homepage: www.elsevier.com/locate/foodchem

Impact of annealing on the molecular structure and physicochemical properties of normal, waxy and high amylose bread wheat starches

H. Lan [a], R. Hoover [a,*], L. Jayakody [a], Q. Liu [b], E. Donner [b], M. Baga [c], E.K. Asare [c], P. Hucl [c], R.N. Chibbar [c]

[a] Department of Biochemistry, Memorial University of Newfoundland, St. John's, NL, Canada A1B 3X9
[b] Guelph Food Research Centre, Agriculture and Agri-Food Canada, 93 Stone Road West, Guelph, ON, Canada N1G 5C9
[c] Department of Plant Sciences and Crop Development Centre, University of Saskatchewan, 51 Campus Drive, Saskatoon, Saskatchewan, Canada S7N 5A8

ARTICLE INFO

Article history:
Received 7 February 2008
Received in revised form 3 April 2008
Accepted 15 April 2008

Keywords:
Starch
Annealing
Wheat
Structure
Properties

ABSTRACT

Starch from normal (CDC teal), high amylose (line 11132) and waxy (99 WAX 27) bread wheat cultivars was isolated and its morphology, composition, structure and properties were studied before and after annealing. Granule diameters, total phosphorus, total amylose, lipid complexed amylose chains, crystallinity, gelatinization temperature range, gelatinization enthalpy, swelling factor (at 90 °C), and amylose leaching (at 90 °C), in the above starches ranged from 2–38 μm, 0.007–0.058%, 26.9–32.3%, 13.4–18.7%, 28.6–42.8%, 12.7–14.3 °C, 11.3–13.3 J/g, 27.6–72.2 and 22.2–26.2%, respectively. Peak viscosity, thermal stability, set-back and susceptibility towards acid hydrolysis followed the order: 99WAX27 > CDC teal > 11132, 11132 > CDC teal > 99WAX27, CDC teal > 99 WAX 27 > 11132, and 99WAX27 > 11132 > CDC teal, respectively. Susceptibility towards α-amylase hydrolysis followed the order: 99 WAX 27 > 11132 > CDC teal (<24 h) and 11132 > CDC teal > 99WAX27 (>24 h). The extent of retrogradation measured by spectroscopy and differential scanning calorimetry followed the order: 11132 > CDC teal > 99WAX27 and 99WAX27 > CDC teal > 11132, respectively. In all starches, concentration of amylose, lipid complexed amylose chains, gelatinization temperature range, swelling factor, amylose leaching, peak viscosity, final viscosity, set-back, light transmission, susceptibility towards α-amylase and acid hydrolysis and the proportion of small (2–8 μm) B-type granules decreased on annealing. Thermal stability and crystallinity increased on annealing. In all starches, gelatinization, enthalpy, retrogradation rate and amylopectin chain length distribution remained unchanged on annealing. Pores and indentations were formed on the granule surfaces of CDC teal and 99WAX27 starches on annealing.

© 2008 Elsevier Ltd. All rights reserved.

1. Introduction

Annealing is a process whereby starch granules in excess (>60% w/w) or at intermediate water content (40% w/w) are held at a temperature above the glass transition temperature (T_g) but below the onset (T_o) temperature of gelatinization for a set period of time (Hoover & Vasanthan, 1994; Jacobs & Delcour, 1998). Annealing has been described as a crystal growth/perfection, diffusion controlled non-equilibrium process (Hoover & Vasanthan, 1994; Jacobs & Delcour, 1998). Annealing of starches has been studied at various starch: water ratios (1:1, 1:3, 1:5) and at temperatures ranging from 40 to 75 °C (Hoover & Manuel, 1996b; Hoover & Vasanthan, 1994; Jacobs et al., 1998a,b,c; Jacobs et al., 1995; Knutson, 1990; Kohyama & Sasaki, 2006; Qi et al., 2004; Tester et al., 1998; Tester et al., 2000; Vermeylen et al., 2006; Waduge et al., 2006). The above studies have shown that annealing results in structural changes within the amorphous and crystalline domains of starch granules. These changes in turn influence granular swelling, amylose leaching, pasting properties, gelatinization parameters and susceptibility towards enzymes and acid. Cereal starches (barley, wheat, rice and maize) are ideal for studying the part played by amylose during annealing, since they could be obtained with amylose contents ranging from 0% to 70%. Of the above cereal starches, only barley (Waduge et al., 2006) and maize (Knutson, 1990; Qi et al., 2004) starches (of varying amylose concentrations) have been subjected to annealing studies. However, these studies have not included the impact of annealing on particle size distribution, amylose concentration, lipid content, amylopectin branch chain length distribution, retrogradation and susceptibility towards α-amylase and acid hydrolysis. Furthermore, with the exception of barley starch (Waduge et al., 2006), changes to the granule surface on annealing has not been documented for other cereal starches. Annealing studies on wheat starch has involved only the normal (21–26% amylose) cultivar (Hoover & Vasanthan, 1994; Jacobs et al., 1998a,b,c; Tester et al., 1998).

Recently, it has been shown that amylose chains take part in the structural organization of amylopectin clusters in native

* Corresponding author. Tel.: +1 709 737 8539; fax: +1 709 737 4000.
E-mail address: rhoover@mun.ca (R. Hoover).

0308-8146/$ - see front matter © 2008 Elsevier Ltd. All rights reserved.
doi:10.1016/j.foodchem.2008.04.055

wheat starches. The extent and nature of this participation being influenced by amylose concentration (Yuryev et al., 2007). All of the above author's have shown that crystalline defects exist within wheat starches due to accumulation of amylose tie chains (refers to portion of macromolecules which connect crystallites and have unordered conformation after leaving a crystallite). In starches, containing crystalline defects, amylose chains are not pulled out into the amorphous lamella and/or amorphous background during structure formation of starch granules. The most significant accumulation of crystalline defects has been observed at amylose concentrations greater than 19.5% (Yuryev et al., 2007). Jenkins and Donald (1995) have also shown by small angle X-ray scattering of normal, waxy and high amylose maize and barley starches, that amylose disrupts the packing of amylopectin crystallites. This suggests, that since structural changes occur within starch crystallites on annealing, the extent of these changes may be influenced to a certain degree by the amount of crystalline defects (high amylose > normal > waxy) in the native starches. Thus, the objective of this study was to understand how changes to morphology, composition, granular swelling, amylose leaching, pasting properties, gelatinization parameters, extent of retrogradation and susceptibility towards enzyme and acid hydrolysis on annealing are influenced by variations in composition and structure among native normal, waxy and high amylose wheat starches.

2. Materials and methods

2.1. Materials

Grain from wheat (*Triticum aestivum* L.) cultivar CDC Teal, line 11132 (lacking starch synthase II polypeptide from A and B genomes) and 99WAX27 (an amylose free wheat line lacking granule bound starch synthase) grown during the summer of 2005 at Saskatoon, Saskatchewan, Canada was used for starch extraction. Isoamylase from *Pseudomonas* sp. was purchased from Megazyme International Ireland Limited, Wicklow, Ireland. All chemicals and solvents were of ACS certified grade.

2.2. Methods

2.2.1. Starch extraction

Starches from the three wheat lines were extracted by wet milling, essentially as described earlier (Abdel-Aal et al., 2002).

2.2.2. Starch granule size determination

The sizes of starch granules from the three wheat lines were analyzed by the following method. Purified starch granules were suspended in 90% (v/v) ethanol. A drop of the starch suspension was spread on a microscope slide and air-dried. The slide was placed on the stage of a research microscope (Zeiss). Images of starch granules were analyzed using an image analyzer that was equipped with image acquisition and processing software (Northern Eclipse 6.0, Empix Imaging Inc. Mississauga, Ontario, Canada). Approximately 5000 granules from each of the starch samples were analyzed. Starch granules were grouped according to their diameters, and the number of starch granules in each group was counted. Plotting the relative number of starch granules against granule diameters produced a starch granule size distribution curve. From this curve the percentage A and B-type starch granules were calculated.

2.2.3. Starch granule morphology

Granule morphology of native and annealed starches was studied by a FEI Quanta 400 environmental scanning electron microscopy (SEM) (Brno, Czech Republic).

2.3. Chemical composition of starch

Quantitative estimation of moisture, ash, nitrogen and starch damage was performed by the standard AACC methods (2000). Starch lipids were determined by the procedures outlined in an earlier publication (Vasanthan & Hoover, 1992). Amylose concentration was determined by a colorimetric method (Chrastil, 1987) and by high performance size exclusion chromatography (Demeke et al., 1999). In order to correct for overestimation of apparent and total amylose concentration, amylose was calculated from a standard curve using mixtures of pure potato amylose and amylopectin (over the range 0–100% amylose). Phosphorous content was determined (before and after defatting with hot propanol–water (3:1 v/v) by the method of Jayakody et al. (2005).

2.4. Amylopectin branch chain length distribution

Isoamylase debranching of whole starch accompanied by high pressure anion exchange chromatography with pulsed amperometric detection (HPAEC-PAD) was used to determine the branch chain length distribution of native and annealed starches (Jayakody et al., 2005).

2.5. X-ray diffraction

Starches for X-ray diffraction measurements were kept in a desiccator over saturated K_2SO_4 (25 °C, aw = 0.98) for 1 week. The hydrated samples (0.5 g dry basis) were packed tightly into an elliptical aluminum holder. X-ray diffractograms of native and annealed starches were obtained with a Rigaku RPT 300 PC X-ray diffractometer (Rigaku-Denki, Co. Tokyo, Japan) with operating conditions of target voltage 40 kV; current 100 mA; scanning range 3–35°; scan sped 2.00°/min; step time 0.9 s; divergence slit width 1.0°; scatter slit width 1.0° and receiving slit width 0.6 mm. The moisture content of the samples was determined before and after scanning. Crystallinity of the native and annealed starches was quantitatively estimated following the method of Nara and Komiya (1983) by using the origin software (Origin-version 6.0, Microcal Inc., Northampton, MA, USA).

2.6. Gelatinization parameters

Gelatinization parameters of native and annealed starches were measured using a Seiko differential scanning calorimeter (DSC 210, Seiko Instruments Inc., Chiba, Japan) equipped with a thermal analysis data station and data recording software. Deionized Water (11 μL) was added with a micro-syringe to starch (3.0 mg) in the DSC pans and the contents were stirred. The pans were then sealed, reweighed and allowed to stand overnight at room temperature before DSC analysis. The scanning temperature range and the heating rates were 25–135 °C at rate of 10 °C/min, then held at 135 °C for 5 min. In all measurements, a thermogram was recorded with an empty aluminum pan as a reference. The transition temperatures reported are the onset (T_o), peak (T_p) and conclusion (T_c). The enthalpy of gelatinization (ΔH) were estimated by integrating the area between the thermogram and a base line under the peak and was expressed in terms of Joules per gram (J/g) of dry starch.

2.7. Swelling factor (SF)

The SF of native and annealed starches when heated to 50–90 °C in excess water was measured according to the method of Tester and Morrison (1990). The SF is reported as the ratio of the volume of swollen granules to the volume of the dry starch. Three replicate samples were used in this determination.

2.8. Amylose leaching (AML)

Starches (20 mg, db) in water (10 mL) were heated at 50–90 °C in volume calibrated sealed tubes for 30 min (tubes were shaken by hand every 5 min to resuspend the starch slurry). The tubes were then cooled to room temperature and centrifuged at 2000g for 10 min. The supernatant liquid (1 mL) was withdrawn and amylose content determined as described by Chrastil (1987). AML was expressed as percentage of amylose leached per 100 g of dry starch. Three replicate samples were used in this determination.

2.9. Pasting properties

A rapid ViscoTM Analyser RVA-4 (Newport Scientific Pty, Ltd., Warriewood, NSW, Australia) was used to determine the pasting properties of starches (7% db, 27 g total weight). Native and annealed starch slurries were equilibrated at 50 °C for 1 min, heated at 6 °C/min to 95 °C, held at 95 °C for 5 min, cooled at 6 °C/min to 50 °C, and held at 50 °C for 2 min. The spindle speed was 960 rpm for the first 10 s (to disperse the sample) and then at 160 rpm for the remainder (~23 min) of the experiment. The reported values are the means of duplicate measurements.

2.10. Enzyme hydrolysis

Enzyme hydrolysis of native and annealed starches were conducted using a crystalline suspension of porcine pancreatic α-amylase in 2.9 M NaCl containing 3 mM $CaCl_2$ (Sigma Chemical Co; St. Louis, MO, USA) in which the concentration of α-amylase was 32 mg protein/mL and the specific activity was 1.122 units/mg protein. Hydrolysis was carried out by the method of Hoover and Vasanthan (1994). The reported values are the means of three replicates.

2.11. Acid hydrolysis

Native and annealed starches were hydrolyzed in triplicate with 2.2 N HCl at 35 °C (1 g starch/40 ml acid) for periods ranging from 1 to 20 days according to the method of Jayakody and Hoover (2002). The extent of hydrolysis was determined by expressing the solubilized carbohydrates as a percentage of the initial starch. Results used for calculation are means of triplicate measurements.

2.12. Retrogradation

The retrogradation characteristics of native and annealed starches was determined by turbidity measurements and by differential scanning calorimetry.

2.12.1. Turbidity measurements

Turbidity was determined by heating a 2% aqueous suspension (pH 7.0) of native and annealed starches at 95 °C for 1 h. The samples were then stored at 4 °C for 24 h (to increase nucleation), followed by 1–19 days at 40 °C. The development of turbidity at the relevant time intervals was followed by measuring the absorbance at 640 nm against a water blank in a UV–vis spectrophotometer.

2.12.2. Differential scanning calorimetry (DSC)

Retrogradation characteristics of native and annealed starches were determined according to the method of Jayakody et al. (2005). The scanning temperature range and heating rate were identical to that used for the study of gelatinization characteristics.

2.13. Annealing

Starches were subjected to one step annealing. Native starch samples (30 g, db) were weighed into glass containers. The starch slurries were prepared with a starch to water ratio of 1:3. The sealed samples were incubated at about 10 °C below the onset temperature (T_o) of gelatinization for 72 h in water bath. At end of the incubation period, samples were centrifuged (2000g) and supernatant was decanted (no amylose or soluble carbohydrates were detected in the supernatant). The annealed starches were washed once with deionized water and air-dried at room temperature.

2.14. Statistical analysis

All determinations were replicated three times, mean values and standard deviations were reported. Analysis of variance (two way ANOVA) was performed by Tukey's HSD test ($P < 0.05$) using Statistical Software SPSS version 14.0 for Windows (SPSS Inc. Chicago, IL, USA).

3. Results and discussion

3.1. Isolation and chemical composition

The data on yield and composition are presented in Tables 1 and 2. The purity of the starches was judged on the basis of composition (low ash (0.03–0.15%) and low nitrogen content (0.02–0.07%)) and microscopic examination (Fig. 1). The average yield of starch from CDC teal, 11132 and 99WAX27 was 45.0%, 38.5% and 48.0%, respectively. The total phosphorus content and non-lipid phosphorus content ranged from 0.007% to 0.058% (1132 > CDC teal > 99WAX27) and 0.007% to 0.034% (CDC teal > 11132 > 99WAX27), respectively (Table 1). The decrease in total phosphorus content of CDC teal and 11132 starches on defatting (Table 2) suggests the presence of lipid phosphorus (in the form of phospholipids) in the above starches. The phosphorus remaining in defatted CDC teal and 11132 starches are mainly in the form of phosphate monoesters and/or inorganic phosphorus. In 99WAX27 starch, phosphorus mainly occurs as non-lipid phosphorus, since the total phosphorus content remained unchanged on defatting (Table 1). The total phosphorus content of CDC teal (0.056%) and that of 11132 (0.058%) were within the range reported by Raeker et al. (1998) for starches from soft wheat cultivars. Amylose concentration was determined colorimetrically (Chrastil, 1987) and by high performance size exclusion chromatography (HPSEC) (Demeke et al., 1999), since the amylose concentration of wheat starch has been found to vary depending upon the method used in its determination (Demeke et al., 1999, Yamamori et al., 1995). The apparent and total amylose concentration determined by Chrastil's method (1987) in which starch is solubilized by sodium hydroxide were 23.28% (CDC teal), 26.87% (CDC teal) and 26.34% (11132), 32.29% (11132), respectively (Table 2). The apparent and total amylose concentrations determined by Chrastil's method (1987) in which starch is solubilized by urea-dimethyl sulfoxide were 23.26% (CDC teal), 26.35% (11132) and 0% (99WAX27), and 26.72% (CDC teal), 32.40% (11132) and 0% (99WAX27), respectively (Table 2). There was no significant difference between the total amylose concentration determined by high performance size exclusion chromatography (26.94% CDC teal, 32.17% (11132), 0% (99WAX27) and that by colorimetry (Table 2). The total amylose concentration of CDC teal and 11132 starches was within the range reported for other varieties of normal (25.7–28.8%) (Yamamori et al., 1995) and high amylose (30–37%) (Hung & Morita, 2006; Yamamori et al., 1995) wheat starches. The free and bound lipid contents (Table 1) ranged from 0.02% to 0.07% (11132 > 99WAX27 ~ CDC teal) and 0.24% to 0.77% (11132 > CDC teal > 99WAX27), respectively. An increase in bound lipid content with increase in amylose concentration has also been reported by Li et al. (2001) for barley starches. There

Table 1
Chemical composition of native and annealed wheat starches[A]

Wheat cultivar	Moisture (%)	Ash (%)	Nitrogen (%)	Total phosphorous (%)[B]	Non-lipid phosphorus (%)[C]	Lipid (%)	
						CM[D]	PW[E]
CDC teal							
Native	9.11 + 0.05[a]	0.15 + 0.01[a]	0.04 + 0.01[a]	0.056 + 0.03[a]	0.034 + 0.06[a]	0.03 + 0.01[a]	0.69 + 0.06[a]
Annealed	10.56 + 0.01[b]	0.15 + 0.01[a]	0.04 + 0.01[a]	0.056 + 0.03[a]	0.034 + 0.06[a]	0.01 + 0.01[a]	0.72 + 0.08[a]
11132							
Native	9.27 + 0.02[a]	0.15 + 0.02[a]	0.07 + 0.02[a]	0.058 + 0.07[a]	0.033 + 0.1[a]	0.07 + 0.02[a]	0.77 + 0.05[a]
Annealed	10.75 + 0.02[b]	0.15 + 0.02[a]	0.07 + 0.02[a]	0.058 + 0.07[a]	0.033 + 0.1[a]	0.03 + 0.01[a]	0.82 + 0.06[a]
99WAX27							
Native	10.44 + 0.03[a]	0.03 + 0.01[a]	0.02 + 0.02[a]	0.007 + 0.10[a]	0.007 + 0.02[a]	0.02 + 0.01[a]	0.24 + 0.01[a]
Annealed	10.50 + 0.04[a]	0.03 + 0.01[a]	0.02 + 0.02[a]	0.007 + 0.10[a]	0.007 + 0.02[a]	0.01 + 0.01[a]	0.25 + 0.02[a]

[A] All data reported on dry basis and represents the mean of three determinations. Means of native and annealed starches of a particular cultivar with different superscripts are significantly different ($p < 0.05$). The average yield of starch isolated from CDC Teal, 11132 and 99WAX27 was 45.0%, 38.5% and 48.0%, respectively.
[B] Determined before removal of free and bound lipids.
[C] Determined after removal of free and bound lipids.
[D] Lipids extracted from native starch by chloroform–methanol (CM) 2:1 (v/v) at 25 °C (mainly free lipids).
[E] Lipids extracted by hot 1-propanol-water (PW) 3:1 (v/v) from the residue left after CM extraction (mainly bound lipids).

Table 2
Amylose concentration of native and annealed wheat starches determined by colorimetry and high performance size exclusion chromatography[A]

Wheat cultivar	Amylose concentration (%)[B]		LCA[F]	Amylose concentration (%)[C]		LCA[F]	Amylose concentration (%)[D]
	Apparent[E]	Total[E]		Apparent[E]	Total[E]		Total[E]
CDC teal							
Native	23.3 + 0.1[a]	26.9 + 0.2[a]	13.9 + 0.4[a]	23.2 + 0.1[a]	26.7 + 0.1[a]	13.4 + 0.1[a]	26.9 + 0.2[a]
Annealed	21.5 + 0.2[b]	24.6 + 0.3[b]	12.8 + 0.3[b]	21.4 + 0.2[b]	24.6 + 0.3[b]	12.5 + 0.1[b]	26.8 + 0.1[a]
11132							
Native	26.3 + 0.1[a]	32.3 + 0.2[a]	18.4 + 0.5[a]	26.4 + 0.2[a]	32.4 + 0.1[a]	18.7 + 0.3[a]	32.2 + 0.1[a]
Annealed	24.5 + 0.2[b]	29.3 + 0.2[b]	16.3 + 0.1[b]	24.3 + 0.1[b]	29.2 + 0.1[b]	16.7 + 0.5[b]	32.7 + 0.1[a]
99WAX27							
Native	–	–		–	–		–
Annealed	–	–		–	–		–

[A] All data reported on dry basis and represents the means of three determinations. Means of native and annealed starches of a particular cultivar with different superscripts are significantly different ($p < 0.05$).
[B] Amylose concentration determined by Chrastil (1987) colorimetric method in which starch was solubilized with NaOH.
[C] Amylose concentration determined by Chrastil (1987) colorimetric method in which starch was solubilized with urea-dimethylsuphoxide.
[D] Amylose concentration determined by high performance size exclusion chromatography.
[E] Apparent and total amylose determined by iodine binding before and after removal of free and bound lipids, respectively.
[F] Lipid complexed amylose chains $(\%) = \frac{\text{total-apparent}}{\text{total}} \times 100$.

were no significant changes in phosphorus (total and non-lipid), nitrogen, ash, and lipid (free and bound) contents on annealing (Table 1). However, the amylose concentration (apparent and total) determined colorimetrically using NaOH and/or urea-DMSO decreased on annealing (Table 2). The extent of this decrease for apparent amylose concentration was in the range 1.87–1.97% (CDC teal) and 1.81–2.06% (11132). Whereas, for total amylose concentration this was in the range of 1.91–2.25% and 1.91–3.24% for CDC teal and 11132, respectively. Determination of total amylose concentration by HPSEC, showed no decrease on annealing in both CDC teal and 11132 starches (Table 2). The iodine-based colorimetric determination of amylose concentration is based on the ability of the amylose helix to interact with pentaiodide (I_5^-) ions. The I_5^- has been shown to be present in the central tunnel of the helix (Teitelbaum et al., 1978). The decrease in total amylose concentration after annealing suggests decreased iodine binding to the amylose helix. Decreased iodine binding could occur if the thermal energy imparted to helical amylose chains had triggered a change in conformation (helix to coil) and/or facilitated interaction (mainly by hydrogen bonding) between amylose–amylose (AM–AM) and/or amylose–amylopectin (AM–AMP) chains. McGrance et al. (1998) have shown that one turn of the helix accommodates one pentaiodide (I_5^-) anion. This suggests that a decrease in the number of helical turns as a result of a change in amylose conformation would decrease the iodine complexing ability of annealed starches. Furthermore, if all the interactions formed between AM–AM and/or AM–AMP chains on annealing were disrupted by sodium hydroxide or by urea-dimethylsulfoxide (reagents used for starch solubilization prior to amylose determination in the Chrastil's (1987) colorimetric method), then the same extent of iodine binding should have occurred in both native and annealed wheat starches. The results suggest that some of the above interactions (especially those between AM–AM chains) may not have been disrupted during starch solubilization. Teitelbaum et al. (1978) have shown that the blue amylose-polyiodide color development is due to rapid and complete formation of the I_5^- complex in short helical segments of amylose which slowly adjust into longer or more ordered helical segments. It is likely that AM–AM and/or AM–AMP interactions formed on annealing could restrict the ability of amylose to form longer or more ordered helical segments, thereby decreasing the color intensity of the amylose–polyiodide complex. Kohyama and Sasaki (2006) have shown by studies on wheat, maize and potato starches that the total amylose concentration remains the same pre and post annealing. However, their method of amylose determination was based on complex formation between concanavalin A (Con A) and amylopectin. In this procedure, the amylopectin in a solubilized lipid free starch sample is precipitated by reaction with Con A and removed by centrifugation. The amylose remaining in the supernatant is then determined after amylolytic hydrolysis to glucose

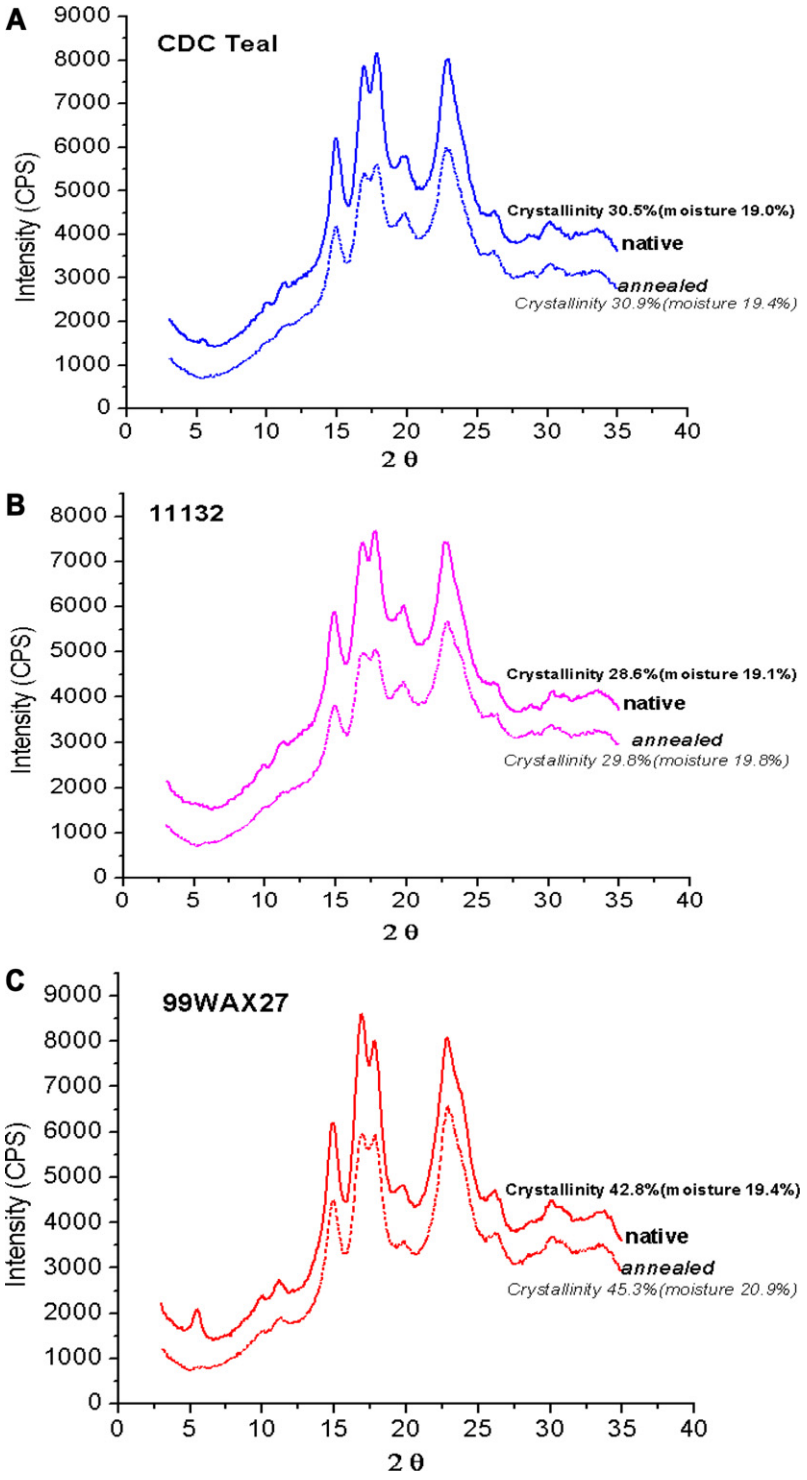

Fig. 1. X-ray patterns and crystallinity of native and annealed CDC Teal (A), 11132 (B) and 99WAX27 (C) starches.

and expressed as a proportion (%) of the glucose derived from amylolytic hydrolysis of the total starch in a separate aliquot of the solubilized sample (prior to Con A treatment).

In our study, HPSEC also showed that amylose concentration remained the same pre and post annealing (Table 2). This was not surprising, since Con A and HPSEC methods of amylose estimation does not rely on iodine binding to the amylose helix. It was interesting to observe, that the percentage of lipid complexed amylose chains (Table 2) also decreased on annealing. This lends support to our postulate that a change in amylose conformation occurs on annealing. A helix to random coil transition would decrease lipid binding. One could then argue that if less amylose–lipid complexes are present after annealing, then the apparent amylose concentration should have theoretically increased after annealing. The results (Table 2) suggests that iodine binding to annealed starches is influenced to a greater extent by changes to amylose conformation and/or to starch chain (AM–AM and/or AM–AMP) interactions, rather by the decreased ability of amylose chains to complex lipids.

3.2. Morphology and granule size distribution

The shape of the large (A-type) and small (B-type) granules of both native and annealed starches were oval to elliptical to round in shape. The granule surfaces of all native starches appeared smooth with no evidence of pores, cracks or indentations. The shape of all granules of CDC teal, 11132 and 99WAX27 remained unchanged on annealing. However, the surfaces of many granules of annealed CDC teal and 99WAX27 starches appeared rough and were covered with pores and indentations. The extent of these changes was more pronounced in the latter. However, the granule surface of 11132 starch remained unchanged on annealing. Waduge et al. (2006) and Hoover and Vasanthan (1994) have shown that the granule morphology (shape and size) and surface characteristics of normal wheat, oat and barley (starches) remains unchanged on annealing. It is difficult to make any comparison between our results and those of the above author's, since the magnification used in their studies (1000x to 3000x) were much lower. In this study, at the above magnifications, no differences were observed in the granule morphology and surface characteristics of native and annealed wheat starches. All three native wheat starches exhibited a bimodal granule size distribution, the two size populations-large and small being termed type-A (>10 μm) and type-B (<10 μm), respectively. The granule diameters ranged from 2 to 38 μm in 99WAX27 and 11132 starches, and from 2 to 36 μm in CDC teal starch. Annealing decreased the proportion of granules having diameters in the range 2–8 μm (CDC teal, 11132) and 2–10 μm (99WAX27). Hung and Morita (2005) have shown by studies on isolated A and B-type granules from normal wheat starch, that at low temperatures (<50 °C), the swelling power of B-type granules are higher than that of A-type granules. This suggests that the decrease in the proportion of small B-types granules on annealing, may have been due to an increase in granular swelling under the annealing conditions (excess water, <50 °C) used in this study. The final granule diameter of the swollen granules may have been set by the annealing temperature.

3.3. Amylopectin branch chain length distribution

The branch chain length distributions of isoamylase – debranched amylopectins of native and annealed starches analyzed by HPAEC-PAD are presented in Table 3. The chains were classified into four groups (dP 6–12, dP 13–24, dP 25–36, dP 37–50). The chain length distribution and the average chain length ($\bar{CL}$) of CDC teal was similar to that of waxy wheat (99WAX27) starch. This suggests that the waxy character has no influence on the chain length distribution profiles of amylopectin molecules (Yasui et al., 1996). However, high amylose (11132) wheat starch exhibited a higher proportion of short chains (dP 6–12) and lower proportions of medium (dP 13–24) and long chains (dP 37–50) than CDC teal and 99WAX27 starches. This suggests that the lack of starch synthase II polypeptide from A and B genomes in 11132 results in shorter A chains (dP 6–12) being synthesized from B_1 chains (dP 13–24) and B3 chains (dP 37–50). The proportion of chains with dP 6–12 (36.5–39.5%) and dP 37–50 (2.5–3.1%) in the wheat starches used in this study was significantly different to that reported (Sasaki et al., 2002; Yasui et al., 1996) for other wheat cultivars. (dP 6–12 (18.9–25.8%), dP > 37 (15.9–23.4%)). Sasaki et al. (2002) have also shown by studies on wheat starches with amylose contents in the range 18.5–28.6, that starches with high amylose content tended to have a higher proportion of short chains (dP 6–12). The amylopectin branch chain length distribution remained unchanged in all three starches on annealing. This suggests that chain length elongation, hydrolysis or debranching of amylopectin chains did not occur on annealing. A similar finding was reported by Kohyama and Sasaki (2006) for potato, corn and normal wheat starches subjected to one step annealing at 20 and 55 °C for 22 h.

3.4. X-ray pattern and crystallinity

The X-ray diffraction patterns of starch granules result from parallel packing of left-handed co-axial double helices in extended regular arrays. Granule crystallinity is believed to result from clustered amylopectin chains of DP 13–15. The X-ray diffraction pattern and crystallinity of native and annealed wheat starches determined at their maximum water absorption capacities are presented in Fig. 1. All three native wheat starches exhibited a predominant A-type X-ray pattern. However, CDC teal and 99WAX27 starches exhibited a peak at 5.5° 2θ (Fig. 1) which is typical for B-type crystallites (Hizukuri et al., 1983). Hizukuri et al. (1983) showed that B-type crystallinity is characteristic of starches with long amylopectin chains. This suggests that the variation in intensity of the peak at 5.5° 2θ (99WAX27 > CDC teal) and the absence of this peak (Fig. 1) in the high amylose (11132) cultivar, reflects differences in average amylopectin chain length (99WAX27 > CDC teal > 11132), and in the proportion of chains with DP > 37 (99WAX27 > CDC teal > 11132). It is highly unlikely that the peak at 5.5° 2θ is influenced by amylose concentration (11132 > CDC teal > 99WAX27), since Vermeylen et al. (2006) have shown the presence of the 5.5° 2θ peak in wheat starches in which the apparent amylose concentration (37.0–37.5%) was much higher than that of 11132 starch (26.3%). Crystallinity of the above starches followed the order: 99WAX27 > CDC teal > 11132 (Fig. 1). Starch

Table 3
Amylopectin chain length distribution of native and annealed wheat starches[A]

Wheat cultivar	Distribution (%)[B]				$\bar{CL}$[D]
	DP 6–12[C]	DP 13–24[C]	DP 25–36[C]	DP 37–50[C]	
CDC teal					
Native	36.51 + 2.05[a]	48.89 + 1.35[a]	11.65 + 0.68[a]	2.95 + 0.02[a]	16.76 + 0.29[a]
Annealed	37.13 + 1.57[a]	48.65 + 0.79[a]	11.79 + 0.53[a]	2.43 + 0.25[a]	16.59 + 0.27[a]
11132					
Native	39.57 + 1.94[a]	45.33 + 1.66[a]	12.53 + 0.46[a]	2.57 + 0.18[a]	16.49 + 0.22[a]
Annealed	40.65 + 1.49[a]	45.27 + 0.64[a]	11.61 + 0.55[a]	2.42 + 0.29[a]	16.25 + 0.30[a]
99WAX27					
Native	35.53 + 2.31[a]	48.85 + 1.34[a]	12.54 + 0.99[a]	3.08 + 0.02[a]	17.00 + 0.33[a]
Annealed	36.01 + 2.24[a]	48.48 + 1.42[a]	12.41 + 0.60[a]	3.11 + 0.18[a]	16.94 + 0.33[a]

[A] All data reported on dry basis and represents the means of three determinations.
[B] DP_n: Indicates degree of polymerization. Total relative area was used to calculate percent distribution.
[C] Means of native and annealed starches of a particular cultivar with different superscripts are significantly different ($p < 0.05$).
[D] Average chain length $\bar{CL}$ calculated by $\Sigma(DP_n \times \text{peak area}_n)/\Sigma(\text{peak area}_n)$.

crystallinity has been shown to be influenced by: (1) amylopectin content, (2) average amylopectin chain length ($\bar{CL}$), (3) orientation of the double helices (within the crystallites) to the X-ray beam, (4) crystallite size and (5) starch moisture content (Abdel-Aal et al., 2002; Jayakody et al., 2005). The higher crystallinity of native 99WAX27 (Fig. 1) starch could be attributed to its higher amylopectin content (Table 2) and longer ($\bar{CL}$) (Table 3). The difference in crystallinity (Fig. 1) between native CDC teal and 11132 starches (CDC teal > 11132) is influenced by the higher amylose content (Table 2), shorter ($\bar{CL}$) (Table 1) and the presence of amylose chains within amylopectin crystallites (this would disrupt the packing of amylopectin crystallites, thereby changing their orientation to the X-ray beam) of 11132 starch. All native starches exhibited a peak at 19.5° 2θ (Fig. 1), which is characteristic of amylose–lipid complexes (Hoover & Hadziyev, 1981). The intensity of this peak followed the order: CDC teal ~11132 > 99WAX27. The nearly similar intensities for CDC teal and 11132 starches was rather surprising, since the amount of lipid complexed chains (Table 2) was much higher in 11132 (18.42–18.70%) than in CDC teal (12.9–13.3%) starch. This suggests that the organization of the amylose–lipid complexes into three dimensional structures (long range order) is probably of a higher order of magnitude in CDC teal starch. The weak amylose–lipid peak exhibited by 99WAX27 starch (Fig. 1) is indicative of weak interaction of lipids with the outer branches of amylopectin. This seems plausible, since 99WAX27 starch is devoid of amylose (Table 2). Annealing changed the X-ray pattern from A + B to a pure A-type pattern in CDC teal and 99WAX27 starches (Fig. 1). However, the A-type X-ray pattern of 11132 starch remained unchanged (Fig. 1). A similar transformation (A + B → A) pattern has also been observed in some varieties of barley (Waduge et al., 2006) starches.

Annealing increased crystallinity (99WAX27 > 11132 > CDC teal) in all starches (Fig. 1). An increase in crystallinity on annealing has also been shown to occur in high amylose barley (Waduge et al., 2006) and normal wheat starches (Hoover & Vasanthan, 1994). An increase in crystallinity on annealing could arise due to the interplay of several factors: (1) An increase in crystal perfection, (2) formation of new crystallites formed by interactions between (AM–AM, AM–AMP, AMP–AMP) starch chains, (3) increase in crystallite size and (4) crystallite reorientation. Consequently, it is difficult to explain the order of increase in crystallinity observed among the wheat starches on annealing. Annealing decreased the intensity of the amylose–lipid complex peak (centered at 19.5°, 2θ) in all starches. This lends credence to our earlier suggestion (based on the data in Table 2) that a change in amylose conformation (helix → coil) occurs on annealing.

3.5. Gelatinization

Starch gelatinization is the disruption of molecular order manifested in irreversible changes in granular properties such as granular swelling, crystallite melting, loss of birefringence and starch solubilization. The gelatinization transition temperatures (onset (T_o), mid-point (T_p), conclusion (T_c), gelatinization transition temperature range (T_c–T_o) and gelatinization enthalpy (ΔH) of native and annealed wheat starches are presented in Table 4. Among the native wheat starches, T_o, T_p, T_c, T_c–T_o and ΔH followed the order: 99WAX27 > CDC teal > 11132. Noda et al. (1996), have shown by studies on wheat and potato starches, that a low T_o, T_p, T_c and ΔH reflect the presence of abundant short amylopectin chains (dP 6–12). This suggests, that the higher proportion of dP 6–12 chains in 11132 starch (Table 3) may have been a factor responsible for its gelatinization parameters (Table 4) being lower than those of CDC teal and 99WAX27 starches (Table 3). Yuryev et al. (2007) have hypothesized that an increase in amylose content leads to an accumulation of amylose "tie-chains" inside both crystalline and amorphous lamella of amylopectin. The chains are single ones that are one-dimensional rigid structures ("string-type") in crystalline lamella, and have an unordered conformation in the amorphous lamella (Yuryev et al., 2007). These "tie-chains" are considered as defects within the crystalline lamella. The most significant accumulation of crystalline defects has been observed at amylose concentrations greater than 19.5% (Yuryev et al., 2007). Protserov et al. (2000) have also shown that an increase in amylose content in starch granules leads to an increase in the extent of crystalline defects and correspondingly, to a decrease in the gelatinization temperature. This suggests that T_o, T_p, T_c and ΔH of CDC teal and 11132 starches are probably influenced by the amount of crystalline defects (11132 > CDC teal). This would also then explain the lower gelatinization parameters for 11132 starch (Table 4). The difference in T_o, T_p, T_c and ΔH between native CDC teal and 99WAX27 starches could be attributed to the presence of crystalline defects in CDC teal starch. This seems plausible, since differences in the proportion of dP 6–12 chains between the two starches was not significant (Table 3). The variation in crystalline stability (T_c–T_o) among the native starches (99WAX27 > CDC teal > 11132) could be attributed to differences in their amylopectin chain ($\bar{CL}$) length (99WAX27 > CDC teal > 11132) (Table 3). In all starches, annealing increased T_o, T_p, T_c and decreased T_c–T_o (Table 4). These changes have been attributed to perfection of pre-existing crystallites (Hoover & Vasanthan, 1994; Jacobs & Delcour, 1998; Knutson, 1990; Tester et al. 1998, 2000; Waduge et al. 2006). The extent of increase in T_o, T_p, and T_c ($T_o > T_p > T_c$)

Table 4
Gelatinization parameters of native and annealed wheat starches[A]

Starch source	Gelatinization transition parameters[A]				
	T_o (°C)[B]	T_p (°C)[B]	T_c (°C)[B]	($T_c - T_o$) (°C)[C]	ΔH (J/g)[D]
CDC teal					
Native	58.3 + 0.2[a]	63.5 + 0.1[a]	72.2 + 0.2[a]	13.9 + 0.2[a]	12.3 + 0.2[a]
Annealed	68.1 + 0.1[b]	71.5 + 0.1[b]	78.5 + 0.1[b]	10.4 + 0.1[b]	12.5 + 0.1[a]
11132					
Native	52.6 + 0.1[a]	57.2 + 0.1[a]	65.4 + 0.1[a]	12.7 + 0.1[a]	11.3 + 0.2[a]
Annealed	61.2 + 0.2[b]	64.3 + 0.5[b]	71.6 + 0.3[b]	10.5 + 0.3[b]	11.0 + 0.1[a]
99WAX27					
Native	59.6 + 0.1[a]	65.5 + 0.2[a]	73.9 + 0.3[a]	14.3 + 0.1[a]	13.3 + 0.2[a]
Annealed	65.0 + 0.1[b]	69.4 + 0.1[b]	76.9 + 0.2[a]	11.9 + 0.2[b]	13.7 + 0.3[a]

[A] All data reported on dry basis and represent the mean + SD of three determinations. Means within each column with different superscripts for native starch and its annealed counterpart are significantly different ($P < 0.05$) by Tukey's HSD test.
[B] T_o, T_p, and T_c represent the onset, peak, and conclusion temperature, respectively.
[C] ($T_c - T_o$) represents the gelatinization temperature range.
[D] ΔH represents the gelatinization enthalpy.

followed the order: CDC teal > 11132 > 99WAX27). Whereas, the extent of decrease in T_c–T_o followed the order: CDC teal > 99WAX27 > 11132 (Table 4). The above orders suggest that crystallites in native CDC teal starch are less perfect than in the other starches. Consequently, the impact of crystalline perfection on T_o, T_p, T_c, and T_c–T_o would be more pronounced in CDC teal starch. The ΔH of all starches remained unchanged on annealing. This suggests that no new double helices were formed on annealing. The constancy of ΔH pre and post annealing has also been reported for maize and barley starches of varying amylose content (Tester et al., 2000; Waduge et al., 2006).

3.6. Amylose leaching (AML) and swelling factor (SF)

Studies on AML and SF provide information on the extent of interaction between starch chains in the amorphous and crystalline domains of the native granule.

The extent of AML and SF at various temperatures are presented in Fig. 2. AML has been shown to be influenced by: (1) total amylose content, (2) extent of interaction between amylose–amylose (AM–AM) and/or amylose–amylopectin (AM–AMP) chains within the native granule, and (3) amount of lipid complexed amylose chains (Hoover & Vasanthan, 1994). In both native CDC teal and 11132 starches, AML, was detected only at temperatures exceeding 70 °C and was most pronounced in the temperature range 80–85 °C. A similar trend has also been reported in barley (Waduge et al., 2006) starches. The higher amount of leached amylose in native 11132 starch could be attributed to its higher total amylose content (Table 2) and/or to weaker interaction between AM–AM and/or AM–AMP chains. It is likely, that the small difference in the extent of AML between native CDC teal and 11132 starches (Fig. 2) is due to the higher content of lipid complexed amylose chains in the latter (Table 2). In both CDC teal and 11132 starches, AML decreased on annealing (Fig. 2a and b). The decrease in AML on annealing has been attributed to: (1) additional interaction between AM–AM and/or AM–AMP chains and (2) increase in the amount of lipid complexed amylose chains (Hoover & Vasanthan, 1994; Tester et al., 2000). In this study, the decreased AML reflects mainly AM–AM and/or AM–AMP interactions, since annealing decreased the amount of lipid complexed amylose chains in both starches (Table 2). The higher extent of AML reduction in CDC teal (Fig. 2a) starch is indicative that amylose chains in native CDC teal starch are probably more compactly packed than in 11132 starch, and are therefore able to interact with other amylose chains more strongly on annealing.

The swelling factor (SF) of native starches followed the order: 99WAX27 > CDC teal > 11132 (Fig. 2c–e). A similar trend has also been reported for maize (Tester et al., 2000) and barley (Waduge et al., 2006) starches. The SF of native 99WAX27 starch increased rapidly in the temperature range 55–65° and thereafter, the SF decreased gradually. The SF of 99WAX27 starch over the temperature range 55–70 °C (Fig. 3) was much higher than that reported for native waxy barley (0% amylose) (Waduge et al., 2006) and waxy maize (0% amylose) (Hoover & Manuel, 1996a) starches.

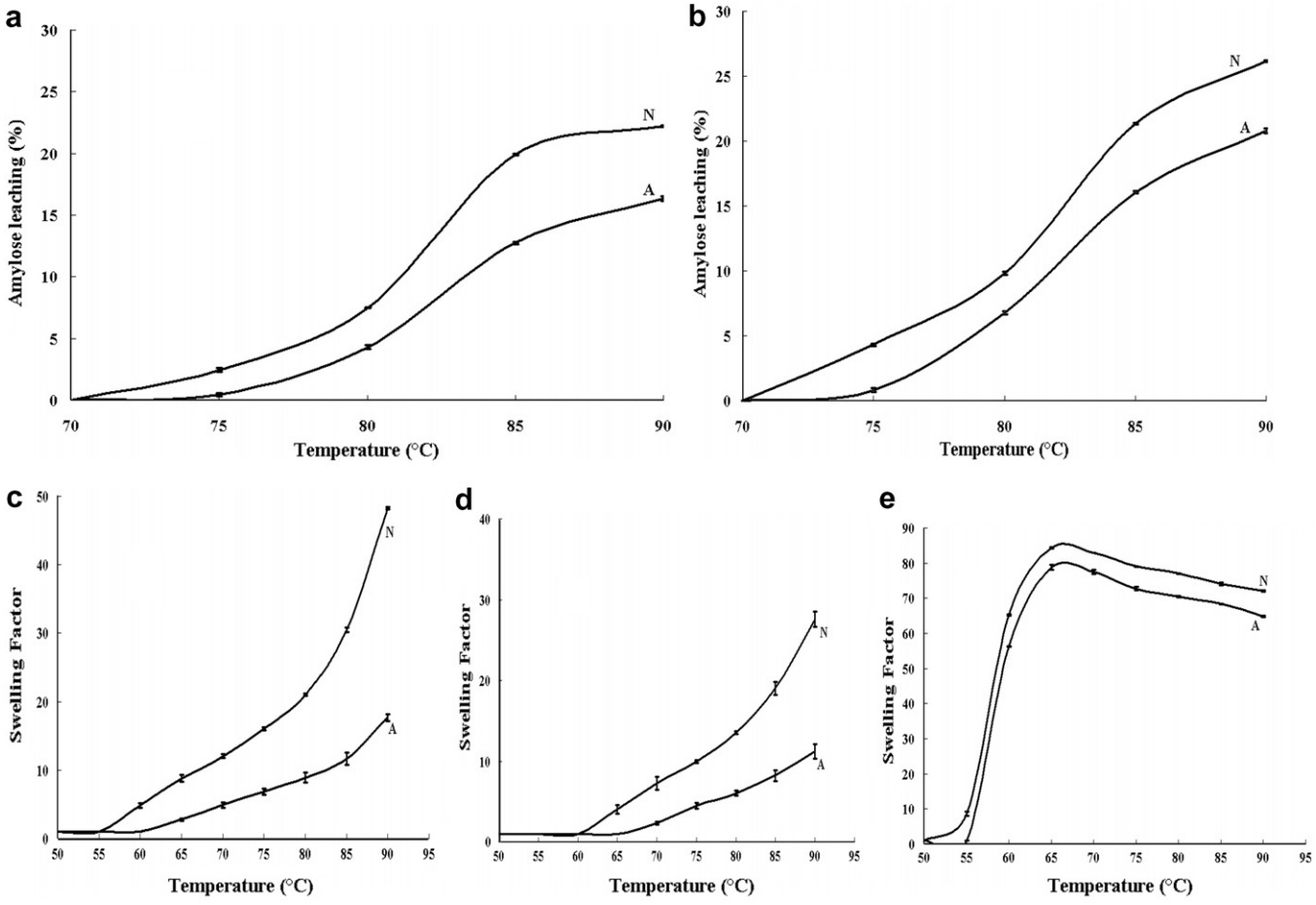

Fig. 2. Amylose leaching in the temperature range 70–90 °C (a) (Native CDC Teal (N)) (Annealed CDC Teal (A)) (b) (Native 11132 (N)) (Annealed 11132 (A)). Swelling factor in the temperature range 50–90 °C. (c) (Native CDC Teal (N)) (Annealed CDC Teal (A)) (d) (Native 11132 (N)) (Annealed 11132 (A)) (e) (Native 99WAX27(N)) (Annealed 99WAX27(A)).

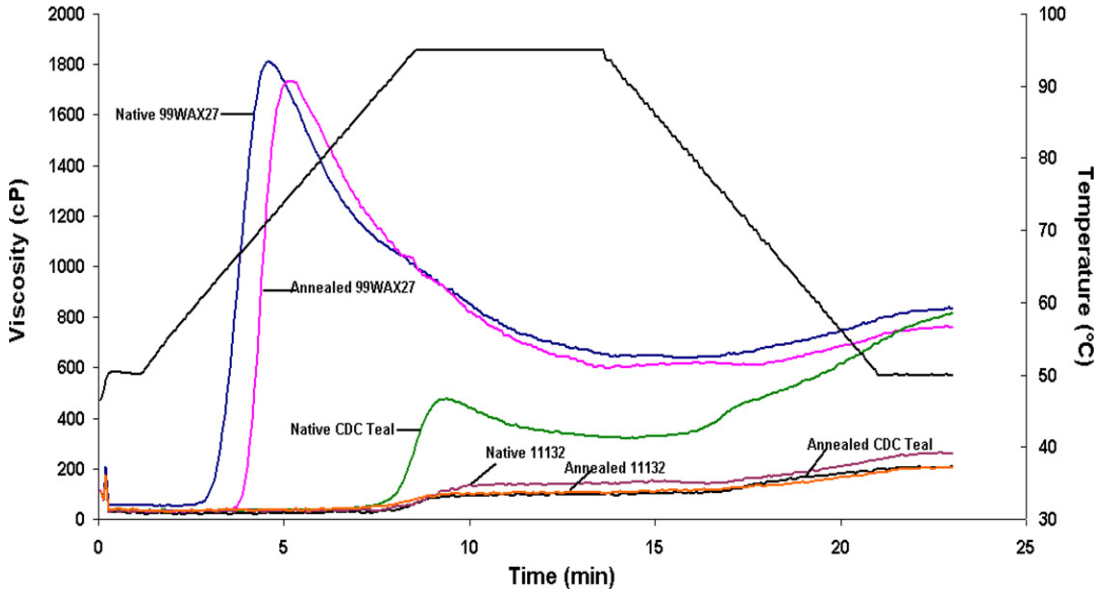

Fig. 3. Pasting curves of native and annealed starches.

For instance, at 70 °C, the SF of native waxy barley (Waduge et al., 2006) and native waxy maize starch (Hoover & Manuel, 1996a) have been reported to be 48 and 22, respectively. In both native CDC teal and 11132 starches, SF increased gradually until 75 °C. Thereafter, the increase in SF (CDC teal > 11132) was more rapid (Fig. 2c and d). A similar trend has also been reported in native normal and high amylose barley (Waduge et al., 2006) and maize (Hoover & Manuel, 1996a) starches. The SF has been shown to be influenced by: (1) amylopectin structure (Sasaki & Matsuki, 1998; Shi & Seib, 1992), (2) V-amylose–lipid complexes (Tester & Morrison, 1990), (3) amylose content (Morrison et al., 1993; Tester et al., 2000) and (4) extent of interaction between AM–AM and/or AM–AMP chains (Hoover & Manuel, 1996a; Tester et al., 2000). Among the native wheat starches, the higher SF of 99WAX27 (Fig. 2e) can be attributed to its higher crystallinity (Fig. 1) and to the absence of amylose–lipid complexes (Table 2). The difference in SF between native CDC teal and 11132 starches (CDC teal > 11132) (Fig. 2c and d) can be attributed to the lower crystallinity (Fig. 1), a more disrupted crystalline structure and to a higher content of lipid complexed amylose chains (Table 2) in the latter.

The SF of all three wheat starches decreased (Fig. 2c–e) on annealing (CDC teal > 11132 > 99WAX27). The SF reduction in the 99WAX27 starch is mainly influenced by the increase in crystalline perfection (Table 4). Whereas, in CDC teal and 11132 starches, in addition to crystalline perfection (Table 4), AM–AM and/or AM–AMP interactions on annealing may have also been responsible for the observed reduction in SF. The extent of this reduction is more pronounced in CDC teal than in 11132 starch, due to greater changes to crystalline perfection (Table 4) and to stronger interaction between AM–AM and/or AM–AMP chains (Fig. 2b and c) in the former on annealing. Reduction in SF on annealing has also been reported in barley (Waduge et al., 2006), oat (Hoover & Vasanthan, 1994) and in commercial normal wheat (Hoover & Vasanthan, 1994) starches.

3.7. Pasting properties

A paste is defined as a viscous mass consisting of a continuous phase (a molecular dispersion) of solubilized amylose and/or amylopectin and a discontinuous phase of granule ghosts and fragments. The changes that occur during gelatinization and pasting greatly affect the rheological properties of the starch suspension. Pasting characteristics are studied by observing changes in viscosity during heating of a starch suspension.

The pasting characteristics of native and annealed wheat starches are presented in Fig. 3. Among the native wheat starches, peak viscosity, extent of viscosity breakdown and the final viscosity followed the order: 99WAX27 > CDC teal > 11132. Whereas, the time taken to reach peak viscosity (peak time) and the degree of set-back followed the order: 11132 > CDC teal > 99WAX27 and CDC teal > 99WAX27 > 11132, respectively. The viscosity development during heating of starch granules with water under shear has been attributed to formation of tightly packed array of swollen deformable granules, friction between swollen granules, amount of leached amylose and amylopectin content (Jacobs et al., 1995; Sasaki et al., 2002). The viscosity rise during cooling of a heated starch suspension has been attributed to interaction between leached amylose chains, granule size and rigid swollen granules (Hoover & Vasanthan, 1994; Jacobs et al., 1995). The higher peak viscosity (PV) exhibited by native 99WAX27 starch is indicative of its higher amylopectin content (Table 2) and higher crystallinity (Fig. 1). Both these factors would enable granules of 99WAX27 to swell rapidly without disintegration (Fig. 3). It is highly unlikely, that amylose leaching (AML) has any significant impact on the PV of native CDC teal and 11132 starches (CDC teal > 11132), since the difference in AML between these two starches was only marginal (Fig. 2a and b). The difference in PV between CDC teal and 11132 starches is more likely due to a higher crystallinity (Fig. 1), higher amylopectin content (Table 2) and to less compactly packed amylose chains in the former (Fig. 2a and b). The extent of viscosity breakdown during the holding cycle is more pronounced in native 99WAX27 (Fig. 3) starch, due to greater susceptibility of the highly swollen granules to shear. The very high resistance of 11132 native starch to shear during the holding cycle (Fig. 3) could be attributed to its lower extent of granule swelling (Fig. 2e) and to a more compact arrangement of amylose chains within the amorphous domains of the granule (Fig. 2b). Jacobs et al. (1995) and Hoover and Vasanthan (1994) have shown that the extent of set-back is influenced by the amount of leached amylose, granule size, and to the presence of unfragmented rigid swollen granules embedded in the leached amylose network. The extent of set-back in the native wheat starches (CDC teal >

99WAX27 > 11132) (Fig. 3) cannot be solely attributed to AML for the following reasons: (1) native 99WAX27 starch exhibits a set-back that is higher (Fig. 3) than that of native 11132 starch, although it is devoid of amylose (Table 2), and (2) 11132 starch exhibits a lower degree of set-back than CDC teal (Fig. 3) although it exhibits a higher degree of AML (Fig. 2a and b). This suggests that set-back in the above native starches is influenced mainly by the interplay between granule size and amylopectin chain length distribution. Among the starches, set-back is more pronounced in native CDC teal due to its higher proportion of large A-type (>10 μm granules). These granules (fragmented or unfragmented) if embedded within the leached amylose matrix, would increase starch viscosity, thereby enhancing the viscosity increase during the cooling cycle. The difference in set-back between native CDC teal and 11132 starches could be attributed to the small proportion of A-type granules and to a higher proportion of amylopectin chains with dP 6–12 (Table 3) in the latter. Chains with dP (6–12) have been shown to hinder association between amylopectin chains (Shi & Seib, 1992). The difference in set-back between native 99WAX27 and 11132 starches (99WAX27 > 11132) could only be attributed to differences in the proportion of long amylopectin chains with dP 37–50 (99WAX27 > 11132) (Table 3), since 99WAX27 starch is devoid of amylose (Table 2) and its proportion of large A-type granules is smaller than in 11132 starch. The higher set-back in 99WAX27 starch (Fig. 3) is indicative of the presence of a more extensively hydrogen bonded network structure formed by interaction between long amylopectin chains (dP 37–50) during the cooling cycle.

Annealing (Fig. 3) decreased PV (CDC teal > 11132 > 99WAX27), breakdown viscosity (CDC teal > 99WAX27 > 11132), final viscosity (CDC teal > 99WAX27 > 11132), set-back (CDC teal > 99WAX27 > 11132) and increased peak time (CDC teal > 99WAX27 > 11132). The decrease in PV on annealing can be attributed to decreased SF (Fig. 2c–e) and AML (Fig. 2a and b). This decrease is more pronounced in CDC teal (Fig. 3), due to greater reductions in AML (Fig. 2a) and SF (Fig. 2c). The increased thermal stability in all starches on annealing (Fig. 3), reflects the decrease in SF (Fig. 2c–e). In CDC teal and 11132 starches, the decrease in set-back (Fig. 3) on annealing is influenced by the decrease in AML (Fig. 2a and b) and SF (Fig. 2c and d). Whereas, in 99WAX27 starch, the main causative factor influencing the decrease in set-back is the decreased SF (Fig. 2e). Jacobs et al. (1995) and Hoover and Vasanthan (1994) showed that in commercial normal wheat starch, peak viscosity and set-back increases on annealing. The annealing parameters used in the above studies were 45 °C/24 h (Jacobs et al. 1995) and 50 °C/72 h (Hoover & Vasanthan, 1994). The discrepancy between our results and those of the above author's may have been due to differences in cultivar, isolation procedures, annealing temperature, annealing time and the temperature and time used for drying the isolated starch.

3.8. α-Amylase hydrolysis

The difference in the extent of α-amylase hydrolysis among the native starches was marginal. During the early stages (<24 h), hydrolysis followed the order: 99WAX27 > 11132 > CDC teal. Whereas, beyond 24 h, the order of hydrolysis was: 11132 > CDC teal > 99WAX27. Small differences in hydrolysis between normal and waxy starches have also been observed in maize, starches (Hoover & Manuel, 1996a). The above results on native maize and wheat starches suggests that amylose content does not play a significant role in influencing α-amylase hydrolysis. We postulate, that it is the interplay of the following factors that influence the difference in susceptibility of normal, waxy and high amylose wheat starches towards α-amylase: (1) granule size (CDC teal > 11132 > 99WAX27) (larger granules will be less susceptible than smaller granules to α-amylase hydrolysis, due to their smaller surface area), (2) crystallinity (99WAX27 > CDC teal > 11132) (glucosidic bonds buried within starch crystallites will not be readily accessible to hydrolysis by α-amylase), (3) extent of disruption of amylopectin clusters (11132 > CDC teal) (the presence of more amylose tie-chains in 11132 starch would disrupt the crystallites, enabling α-amylase easy access to the glucosidic bonds), (4) lipid complexed amylose chains (11132 > CDC teal > 99WAX27) (glycosidic bonds of lipid complexed amylose chains will be less accessible to α-amylase hydrolysis than those of free amylose chains, since the ability to undergo the chair to half chair conformational change will be difficult, if amylose chains are rendered immobile by the presence of lipid molecules inside their hydrophobic core).

Annealing decreased the extent of α-amylase hydrolysis in CDC teal and 11132 starches (CDC teal > 11132). However, in 99WAX27 starch, susceptibility towards α-amylase increased slightly on annealing. Decreased α-amylase hydrolysis an annealing has also been reported by Hoover and Vasanthan (1994) in commercial normal wheat starch. The decreased hydrolysis on annealing in CDC teal and 11132 (CDC teal > 11132) starches could be explained as being due to increased crystalline perfection (CDC teal > 11132 (Table 4) and to an increase in the proportion of larger A-type granules (CDC teal > 11132). SEM micrographs showed the presence of pores on the granule surface of CDC teal on annealing. Theoretically, formation of pores on granule surfaces should facilitate entry of α-amylase into the granule interior, thereby enhancing hydrolysis. Therefore, the decreased susceptibility of CDC teal starch towards α-amylase on annealing, suggests that the increase in granule size and crystalline perfection (Table 4) may have negated the effect of pore formation on hydrolysis. In 99WAX27 starch, the extent of increase in crystalline perfection (Table 4) and granule size was much lower than in the other two starches. However, more pores were formed on the granule surface of 99WAX27 starch on annealing. This suggests that the marginal increase in hydrolysis in 99WAX27 starch on annealing is due to pore formation negating the effect of increased crystalline perfection and granule size on the extent of hydrolysis. It is difficult to find a consensus of the action pattern of α-amylase on annealed wheat starches (Jacobs et al., 1998b; Wang et al., 1997; Hoover & Vasanthan, 1994) due to differences in α, amylase source and cultivar differences. Furthermore, the above studies have not included waxy and high amylose wheat starches.

3.9. Acid hydrolysis

The extent of acid (2.2 N HCl) hydrolysis among the native starches followed the order: 99WAX27 > 11132 > CDC teal. A relatively slow rate was observed during the first three days, followed by a faster rate between day 4 and day 20. The highest rate of hydrolysis for all three starches occurred between the 12th and 20th day. Acid hydrolysis has been shown to exhibit two phases in barley (Waduge et al., 2006), maize (Jayakody & Hoover, 2002) and wheat (Jacobs et al., 1998c; Tester et al., 1998; Hoover & Vasanthan, 1994) starches. The first phase as been attributed to the relatively fast hydrolysis within the amorphous lamellae, and the second slow phase (between day 9 and day 15) to hydrolysis of the crystalline lamella.

In this study, none of the wheat starches exhibited a slow rate of hydrolysis between day 9 and day 15. This is indicative, that the crystalline regions of the above starches were not hydrolyzed during the time course of hydrolysis. Differences in the extent and rate of hydrolysis among starches has been attributed to the interplay of many factors: (1) granule size (Vasanthan & Bhatty, 1996), (2) lipid complexed amylose chains (Morrison et al., 1993), (3) extent of interaction between starch chains in the amorphous domains (Hoover & Manuel, 1996a), (4) amylopectin chain length distribu-

tion (Srichuwong et al., 2005), (5) pores on the granule surface (Jayakody & Hoover, 2002) and (6) amylose content (Hoover & Manuel, 1996a). Our results indicate that the difference in the extent of hydrolysis among the native wheat starches is largely influenced by differences in their proportion of A-type (large) granules (CDC teal > 11132 > 99WAX27). Granules of 99WAX27 starch are hydrolyzed faster, since the surface area accessible to acid is much larger (due to lower proportion of large A-type granules). It is likely, that differences in granule size may have negated the effect of lipid complexed amylose chains (11132 > CDC teal > 99WAX27), crystallite disruption (11132 > CDC teal) amylose content (11132 > CDC teal > 99WAX27) and proportion of dP 6–12 chains (11132 > CDC teal > 99WAX27) on the rate and extent of acid hydrolysis in the native starches.

In all annealed starches, the extent of acid hydrolysis between day 1 and day 5 were marginally higher than those of their native counterparts. Between day 6 and day 20, all annealed starches were hydrolyzed to a lesser extent than their native counterparts. The extent of this decrease between day 6 and day 8 was marginal and nearly similar for all starches. However, beyond day 9, differences in hydrolysis between native and annealed starches were more pronounced and followed the order: CDC teal > 11132 > 99WAX27. The effect of annealing on the acid hydrolysis profile of normal wheat starches from other cultivars has been shown to be different to that reported in this study. For instance, Tester et al. (1998) showed that during the rapid phase of hydrolysis (2 M HCl at 35 °C/10 days), annealed normal wheat starch was more extensively degraded than its native counterpart, while during the slow phase of hydrolysis, there was no difference. Hoover and Vasanthan (1994) reported a slight reduction (~5%) in hydrolysis on annealing (2.2 M HCl, 35 °C/20 days) normal wheat starch during both phases. Jacobs et al. (1998c) reported no difference in hydrolysis (2.2 M HCl, 35 °C, 20 days) between native and annealed normal wheat starch. In barley starches (normal, waxy and high amylose) the extent of decrease in annealing throughout the time course of hydrolysis has been shown to be less than 5% (Waduge et al., 2006). The extent of decrease in acid hydrolysis on annealing has been attributed to: (1) perfection of starch crystallites, (2) increased resistance of α $(1 \rightarrow 6)$ branch points, (3) formation of V-amylose lipid complexes and (4) formation of amylose double helices (Hoover & Vasanthan, 1994; Jacobs & Delcour, 1998a). Jacobs and Delcour (1998a) have postulated, that perfection of starch crystallites during annealing, causes some of α $(1 \rightarrow 6)$ branch points in the amorphous regions to become more embedded in the crystalline structure, and as a result, less susceptible to acid hydrolysis. The results suggest, that the extent of decrease in acid hydrolysis on annealing is a reflection on: (1) the amount of α $(1 \rightarrow 6)$ branch points that may have become embedded within the starch crystallites (greater in CDC teal, due to larger differences in crystalline perfection between, the native and annealed states (Table 4), and (2) the extent of interaction between AM–AM chains (greater in CDC teal (Fig. 3)). It is highly unlikely, that acid hydrolysis is influenced by the amount of lipid complexed amylose chains (LCAC), since LCAC decreased on annealing (Table 2).

3.10. Retrogradation

Retrogradation occurs when the starch components in gelatinized starch reassociate in an ordered structure. In its initial phase, two or more glucan chains may form a simple juncture point, which may then develop into more extensively ordered regions. Ultimately, under favorable conditions, a crystalline order appears. In this study, retrogradation of the wheat starches was determined by turbidity and DSC measurements.

3.10.1. Transmission measurements

The percentage light transmission (%*T*) of the native starches followed the order: 99WAX27 > CDC teal > 11132 throughout the storage period. In the native starches, %*T* of CDC teal and 99WAX27 starches decreased gradually during storage. However, 11132 starch exhibited a steep decrease in %*T* at the end of the third day of storage followed by a gradual decrease thereafter. At the end of the storage period (17 days), %*T* had decreased by 15.3%, 52.6% and 14.8% in native CDC teal, 11132 and 99WAX27 starches, respectively. This suggests that the extent of retrogradation is most pronounced in native 11132 starch.

In all starches, %*T* decreased on annealing (CDC teal > 11132 > 99WAX27). In both annealed CDC teal and 11132 starches, the change in %*T* was most pronounced at the end of the third day of storage. At the end of the 17th day, %*T* had decreased by 43.6%, 32.8% and 22.7% in annealed CDC teal, 11132 and 99WAX27 starches, respectively. This suggests that among the annealed starches, retrogradation is most pronounced in CDC teal starch.

Retrogradation occurs when the starch components in gelatinized starch reassociate in an ordered structure. In its initial phase, two or more glucan chains may form a simple juncture point, which may then develop into more extensively ordered regions. Ultimately, under favourable conditions, a crystalline order appears.

The extent of %T have their origin in refractive index fluctuation over a distance scale comparable to the wavelength of observation. In a polymer solvent system this is caused by density fluctuation over the same distance scale and has been attributed to polymer–polymer aggregation (Gidley & Bulpin, 1989). Gidley and Bulpin (1989) have shown, on the basis of their studies on amylose aggregation in aqueous systems, that even at the onset of detectable transmission, highly aggregated polymer structures are present, Craig et al. (1989) have classified starch pastes into three categories depending on the behavior in light: (1) high clarity and almost no whiteness due to little or no refraction of light resulting from lack of swollen granule remnants and little reflection of light (due to limited association of starch chains), (2) moderate clarity and high whiteness due to little refraction (few granular remnants) and high reflection of light (due to interaction between polymer chains), and (3) low clarity and low whiteness (due to high refraction of light by swollen granular remnants but little reflection by collapsed or associated starch granules). SF measurements (Fig. 2) showed the highest granular swelling for native 99WAX27 (Fig. 2e) starch. This suggests that granule remnants may not have been present during transmission measurements (since the granules of 99WAX27 starch would have been very fragile and thus prone to extensive disintegration). This would then partly explain the high %*T* of native 99WAX27 starch during the storage period. In addition, weak interaction between amylopectin chains of 99WAX27 starch during storage may have also accounted for its high %*T*. The difference in %*T* between native CDC teal and 11132 starches (CDC teal > 11132) could be attributed to the greater extent of amylose leaching (Fig. 2a and b) and to the presence of more intact granule remnants in the latter (since the SF of 11132 (Fig. 2b) starch was less than that of CDC teal starch (Fig. 2a)). It is also likely, that interactions between amylose chains may have been more pronounced in 11132 starch (due to a greater extent of amylose (Fig. 2b) leaching) than in CDC teal starch (Fig. 2a). This would then also explain the difference in %*T* between these two starches. The steeper reduction in %*T* during the first three days of storage in CDC teal and 11132 starches is indicative of rapid amylose–amylose interactions and/or binding of granule remnants into assemblies by leached amylose and amylose aggregates. The plateaued %*T* after five days storage in CDC teal and 11132, starches, and after nine days storage in 99WAX27 starch corresponds to slow aggregation of amylose–amylose and amylopectin–amylopectin chains.

The reduction in %*T* on annealing reflects reduction in SF (Fig. 2c–e). A reduction in SF would make the granules less fragile, and thus increase the amount of intact granule remnants. The effect of reduction in %*T* on annealing is more pronounced in CDC teal starch, since the extent of reduction in SF on annealing followed the order: CDC teal > 11132 > 99WAX27 (Fig. 2c–e). The results showed that the rate of retrogradation (determined by noting the extent of decrease in %*T* at the various time intervals of storage) of annealed CDC teal and 11132 starches were lower (due to a decrease in amylose (Fig. 2a and b) leaching) than that of their native counterparts. Whereas, in 99WAX27 starch, annealing increased the rate of retrogradation. The effect of annealing on the rate of retrogradation of waxy (99WAX27) and amylose containing starches (CDC teal, 11132) can be explained by considering the changes that occur within the crystalline lamella during gelatinization. Waigh et al. (2000) have postulated that during gelatinization in excess water, the double helices forming the crystalline lamella undergo slow side by side dissociation, followed by a fast helix to coil transition. DSC results (Table 4) showed that crystalline perfection occurs on annealing. This suggests that the extent of dissociation and unraveling of the double helices during gelatinization would be slower in annealed starches. Consequently, during gel storage, the formation and lateral association of the unraveled double helices would be faster in annealed than in native starches. This would then explain the difference in the rate of retrogradation between native and annealed (annealed > native) 99WAX27 starches. The difference in the rate of retrogradation between native and annealed (native > annealed) CDC teal and 11132 starches, suggests that in the annealed starches, reduced amylose leaching (Fig. 2) negates the faster rate of recrystallization of amylopectin double helices.

3.10.2. DSC measurements

The enthalpy (ΔH_R) of retrogradation (mainly represents the dissociation, unraveling and melting of the double helices formed by associations between the outer A-chains of amylopectin during storage) of the native starches at the 2nd and 7th day of storage at 40 °C, followed the order: 99WAX27 > CDC teal > 11132. The rate of retrogradation (determined by the increase in ΔH_R between the 2nd and 7th day of storage followed the order: 99WAX27 > CDC teal > 11132. Differences in ΔH_R among starches have been explained on the basis of amylopectin unit chain length distribution (Shi & Seib, 1992) and phosphate monoester content (Jane et al., 1996). Wursch and Gumy (1994) postulated that an increase in molar proportion of unit chains with dP 6–9 inhibits retrogradation. Whereas, an increased molar proportion of unit chains with dP 13–24 increases the extent of retrogradation. Sasaki and Matsuki (1998) showed by studies on wheat starches of amylose content in the range 24.8 to 34.2, that ΔH_R is also influenced by long amylopectin chain lengths (dP > 35). They postulated that a higher proportion of longer chains might form more stable crystallites and more regions of crystallinity during storage. As shown earlier (Table 3), among the native starches, dP 6–12, dP 13–24 and dP > 37–50 followed the order: 11132 > CDC teal > 99WAX27, CDC teal ~ 99WAX27 > 11132 and 99WAX27 > CDC teal > 11132, respectively. This would then explain partly the differences in ΔH_R among the native starches. Jane et al. (1996) have shown that starch phosphate monoesters slow retrogradation due to repulsion between negative charges. Thus, if starch phosphate monoester content was the sole factor influencing differences in ΔH_R among the native starches, then ΔH_R should have followed the order: 99WAX27 > CDC teal ~ 11132 (since starch phosphate monoester content followed the order (CDC teal ~ 11132 > 99WAX27 Table 1). The observed ΔH_R differences among the native starches suggests that the magnitude of ΔH_R is influenced by the interplay between amylopectin unit chain length distribution and starch phosphate monoester content. The differences in the rate of increase in ΔH_R among the native starches (99WAX27 > CDC teal > 11132) reflects differences in their amylopectin content (99WAX27 > CDC teal > 11132).

Annealing had no significant impact on ΔH_R. This was expected, since all interactions formed during annealing would have been disrupted during gelatinization. The extent of increase in ΔH_R in the annealed starches, between the 2nd and 7th day of storage, followed the same trend as their native counterparts.

4. Conclusion

The results showed that changes to physicochemical properties of normal, waxy and high amylose wheat starches on annealing, are influenced by changes to amylose conformation (helix to coil), increase in crystalline perfection, enhanced interaction between starch chains, decrease in the proportion of small B-type granules, and by native starch structure (crystalline defects, amylopectin chain length distribution, amylose concentration, degree of association between starch chains within the amorphous and crystalline domains of the granule).

Acknowledgements

One of the author's (R. Hoover) thanks the Natural Science and Engineering Research Council of Canada for a discovery grant.

References

Abdel-Aal, E. S. M., Hucl, P., Chibbar, R. N., Han, H. L., & Demeke, T. (2002). Physicochemical and structural characteristics of flours and starches from waxy and nonwaxy wheats. *Cereal Chemistry, 78*, 458–464.

American Association of Cereal Chemists. (2000). *Approved methods of the AACC* (10th ed.). MN: St. Paul.

Chrastil, J. (1987). Improved colorimetric determination of amylose in starches or flours. *Carbohydrate Research, 159*, 154–158.

Craig, S. A. S., Maningat, C. C., Seib, P. A., & Hoseney, R. C. (1989). Starch paste clarity. *Cereal Chemistry, 66*, 173–182.

Demeke, T., Hucl, P., Abdel-Aal, E.-S. M., Båga, M., & Chibbar, R. N. (1999). Biochemical characterization of the wheat waxy A protein and its effect on starch properties. *Cereal Chemistry, 76*, 694–698.

Gidley, M. J., & Bulpin, P. V. (1989). Aggregation of amylose in aqueous systems: The effect of chain length on phase behavior and aggregation kinetics. *Macromolecules, 22*, 341–346.

Hizukuri, S., Kaneko, T., & Takeda, Y. (1983). Measurement of the chain length of amylopectin and its relevance to the origin of crystalline polymorphism of starch granules. *Biochemica Biophysica Acta, 760*, 188–191.

Hoover, R., & Hadziyev, D. (1981). Characterization of potato starch and its monoglyceride complexes. *Starch, 33*, 290–300.

Hoover, R., & Manuel, H. (1996a). The effect of heat-moisture treatment on the structure and physicochemical properties of normal maize, waxy maize, dull waxy maize and amylomaize V starches. *Journal of Cereal Science, 23*, 153–162.

Hoover, R., & Manuel, H. (1996b). The effect of annealing on the physicochemical properties of legume starches. In G. R. Fenwick, G. Hedley, R. L. Richards, & S. Kokhar (Eds.), *Agri-food quality: An interdisciplinary approach* (pp. 157–161). Cambridge, UK: The Royal Society of Chemistry.

Hoover, R., & Vasanthan, T. (1994). The effect of annealing on the physicochemical properties of wheat, oat, potato and lentil starches. *Journal of Food Biochemistry, 18*, 67–82.

Hung, V. P., & Morita, N. (2005). Physicochemical properties of hydroxypropylated and cross-linked starches from A-type and B-type wheat starch granules. *Carbohydrate Polymers, 59*, 239–246.

Hung, V. P., & Morita, N. (2006). Waxy and high amylose wheat starches and flour characteristics functionality and application. *Trends in Food Science and Technology, 17*, 448–456.

Jacobs, H., Mischenko, N., Koch, M. H. J., Eerlingen, R. C., Delcour, J. A., & Reynaers, H. (1998a). Evaluation of the impact of annealing on gelatinization at intermediate water content of wheat and potato starches: A differential scanning calorimetry and small angle X-ray scattering study. *Carbohydrate Research, 306*, 1–10.

Jacobs, H., Eerlingen, R. C., Spaepen, H., Grobet, P. J., & Delcour, J. A. (1998b). Impact of annealing on the susceptibility of wheat, potato and pea starches to hydrolysis with pancreatin. *Carbohydrate Research, 305*, 193–207.

Jacobs, H., Eerlingen, R. C., Rouseu, N., Colonna, P., & Delcour, J. A. (1998c). Acid hydrolysis of native and annealed wheat, potato and pea starches. DSC melting features and chain length distribution of lintnerized starches. *Carbohydrate Research, 308*, 359–371.

Jacobs, H., Eerlingen, R. C., Clauwaert, W., & Delcour, J. A. (1995). Influence of annealing on the pasting properties of starches from varying botanical sources. *Cereal Chemistry, 72*, 480–487.

Jacobs, H., & Delcour, J. A. (1998). Hydrothermal modifications of granular starch, with retention of the granular structure. *A review Journal of Agricultural Food Chemistry, 46*, 2895–2905.

Jane, J. L., Kasemsuwan, T., Chen, F., & Juliano, P. O. (1996). Phosphorus in rice and other starches. *Cereal Foods World, 41*, 827–832.

Jayakody, L., & Hoover, R. (2002). The effect of lintnerization on cereal starch granules. *Food Research International, 35*, 665–680.

Jayakody, L., Hoover, R., Liu, Q., & Weber, E. (2005). Studies on tuber and root starches. I. Structure and physicochemical properties of innala (*Solenostemon rotundifolius*) starches grown in Sri Lanka. *Food Research International, 38*, 615–629.

Jenkins, P. J., & Donald, A. M. (1995). The influence of amylose on starch granule structure. *International Journal of Biological Macromolecules, 17*, 315–321.

Knutson, C. A. (1990). Annealing of maize starches at elevated temperatures. *Cereal Chemistry, 67*, 376–384.

Kohyama, K., & Sasaki, T. (2006). Differential scanning calorimetry and a model calculation of starches annealed at 20 and 50 °C. *Carbohydrate Polymers, 63*, 82–88.

Li, J. H., Vasanthan, T., Rossnagel, B., & Hoover, R. (2001). Starch from hull-less barley I. Granule morphology, composition and amylopectin structure. *Food Chemistry, 74*, 395–405.

McGrance, S. J., Cornell, H. J., & Rix, J. C. (1998). A simple and rapid colorimetric method for the determination of amylose in starch products. *Starch, 50*, 158–163.

Morrison, W. R., Tester, R. F., Gidley, M. J., & Karkalas, J. (1993). Resistance to acid hydrolysis of lipid complexed amylose and lipid free amylose in lintnerized waxy and non waxy barley starch. *Carbohydrate Research, 245*, 289–302.

Nara, S., & Komiya, T. (1983). Studies on the relationship between water saturated state and crystallinity by the diffraction method for moistened potato starch. *Starch, 35*, 407–410.

Noda, T., Takahata, Y., Sato, T., Ikoma, H., & Mochida, H. (1996). Physicochemical properties of starches from purple and orange fleshed sweet potato roots at two levels of fertilizer. *Starch, 48*, 395–399.

Protserov, V. A., Karpov, V. G., Kozhevnikov, G. O., Wasserman, L. A., & Yuryev, V. P. (2000). Changes of thermodynamic and structural properties of potato starches (Udacha and Acrosil) varieties during biosyntheses. *Starch, 52*, 461–466.

Qi, X., Tester, R. F., Snape, C. E., Yuryev, V., Wasserman, L. A., & Ansell, R. (2004). Molecular basis of the gelatinization and swelling characteristics of waxy barley starch grown in the same location during the same season. Part II. Crystallinity and gelatinization characteristics. *Journal of Cereal Science, 39*, 57–66.

Raeker, M. O., Gaines, C. S., Finney, P. L., & Donelson, T. (1998). Granule size distribution and chemical composition of starches from twelve soft wheat cultivars. *Cereal Chemistry, 75*, 721–728.

Sasaki, T., Yasui, I., Matsuki, J., & Satake, T. (2002). Comparison of physical properties of wheat starch gels with different amylose content. *Cereal Chemistry, 79*, 861–866.

Sasaki, T., & Matsuki, J. (1998). Effect of wheat starch structure on swelling power. *Cereal Chemistry, 75*, 525–529.

Shi, Y. C., & Seib, P. A. (1992). The structure of four waxy starches related to gelatinization and retrogradation. *Carbohydrate Research, 227*, 131–145.

Srichuwong, S., Isono, N., Mishima, T., & Hisamatsu, M. (2005). Structure of lintnerized starch is related to X-ray diffraction patterns and susceptibility to acid and enzyme hydrolysis of starch granules. *International Journal of Biological Macromolecules, 37*, 115–121.

Teitelbaum, R. C., Ruby, S. L., & Marks, T. J. (1978). On the structure of starch-iodine. *Journal of the American Chemical Society, 100*, 3215–3217.

Tester, R. F., Debon, S. J. J., & Karkalas, J. (1998). Annealing of wheat starch. *Journal of Cereal Science, 28*, 259–272.

Tester, R. F., Debon, S. J. J., & Sommerville, M. D. (2000). Annealing of maize starch. *Carbohydrate Polymers, 47*, 287–299.

Tester, R. F., & Morrison, W. R. (1990). Swelling and gelatinization of cereal starches. I. Effects of amylopectin, amylose and lipids. *Cereal Chemistry, 67*, 551–557.

Vasanthan, T., & Hoover, R. (1992). Effect of defatting on starch structure and physicochemical properties. *Food Chemistry, 45*, 337–347.

Vasanthan, T., & Bhatty, R. S. (1996). Physicochemical properties of small and large granule starches of waxy, regular and high amylose barley. *Cereal Chemistry, 73*, 199–207.

Vermeylen, R., Goders, B., & Delcour, J. A. (2006). An X-ray study of hydrothermally treated potato starch. *Carbohydrate Polymers, 64*, 364–375.

Waduge, R. N., Hoover, R., Vasanthan, T., Gao, J., & Li, J. (2006). Effect of annealing on the structure and physicochemical properties of barley starches of varying amylose content. *Food Research International, 39*, 59–77.

Waigh, T. A., Kato, K. L., Donald, A. M., Gidley, M. J., Clarke, C. J., & Riekel, C. (2000). Side-chain liquid-crystalline model for starch. *Starch, 52*, 450–460.

Wang, W. J., Powell, A. D., & Oates, C. G. (1997). Effect of annealing on the hydrolysis of sago starch granules. *Carbohydrate Polymers, 33*, 195–202.

Wursch, P., & Gumy, D. (1994). Inhibition of amylopectin by partial beta-amylolysis. *Carbohydrate Research, 256*, 129–133.

Yamamori, M., Nakamura, T., & Nagamine, T. (1995). Inheritance of waxy endosperm character in a common wheat lacking 3 Wx proteins. *Breeding Science, 45*, 377–379.

Yasui, T., Matsuki, J., Sasaki, T., & Yamamori, M. (1996). Amylose and lipid contents, amylopectin structure, and gelatinization properties of waxy wheat (*Triticum aestivum*) starch. *Journal of Cereal Science, 24*, 131–137.

Yuryev, V. P., Kozlov, S. S., Noda, T., Bertoft, E., & Blennow, A. (2007). Influence of different GBSS1 and GWD combinations on the amylose localization within wheat and potato starch granules. In Yuryev et al. (Eds.), *Starch: Achievements in understanding of structure* (pp. 1–47). Nova Science Publishers Inc.